**DATA REPOSITORY ITEM 2010107**

Sub-Milankovitch solar forcing of past climates:

mid and late Holocene perspectives

**Samuli Helama[1], Marc Macias Fauria[2], Kari Mielikäinen[3], Mauri Timonen[4], Matti Eronen[1]**

[1]*Department of Geology, P.O. Box 64, 00014 University of Helsinki, Finland*

[2]*Biogeoscience Institute, University of Calgary, Canada*

[3]*Finnish Forest Research Institute, Vantaa Research Unit, Finland*

[4]*Finnish Forest Research Institute, Rovaniemi Research Unit, Finland*

## MATERIAL AND METHODS

### Introduction

Disappointingly low amounts of millennial climate variations have been recorded so far in tree-ring–derived paleoclimatic reconstructions. This scarcity has two causes: an lack of multi-millennial tree-ring chronologies in general and the difficulties of dendrochronological techniques to extract information about millennial climate variations from tree rings, in particular. In fact, previous studies (Cook et al., 1995; Briffa et al., 1996; Helama et al., 2004c) have suggested that many of the commonly accepted and used techniques in dendrochronological studies virtually efface much of the climatic variation at the multi-centennial and potentially longer timescales. In other words, the “low-frequency” portion of the paleoclimatic spectrum is lost.

These issues present a conundrum. If tree rings can be used to reconstruct millennial solar variations, then why would the same proxy fail to reconstruct similar variations in simple climatic parameters such as temperature? The answer can be directly found from the specific wood component that is used to build the records. While sunspot numbers can be traced back in time using isotopic composition ($\Delta^{14}C$) in wood (Stuiver et al., 1998), paleoclimatic reconstructions are largely based on values of radial growth, i.e., tree-ring width or density (Cook et al., 1995; Briffa et al., 1996; Esper et al., 2002) with variations constrained by an array of biological factors involved in the wood-forming process (Fritts, 1976; Vaganov et al., 2006). Consequently, no dendroclimatic interpretation can be carried out before these biological variations have been removed from tree-ring width and density series. The most crucial issue in this respect is the life-long trend in the tree rings of individual trees and how to eliminate it without inadvertently removing climatically excited variations at timescales similar to or longer than the tree lifespan. As previously demonstrated (Cook et al., 1995; Briffa et al., 1996), conventional tree-ring techniques have failed in this particular goal; meanwhile, this failure remains a potential reason for the shortage of low-frequency paleoclimate signals in reconstructions based on tree rings.

Because trees produce narrower rings with increasing age, this trend also arises in part from the ageing process (Fritts, 1976; Vaganov et al., 2006). It has been suggested that a population-wise ontogenetic trend could thus be determined by a single curve as a smoothed average of all available tree-ring series of the same species and environment (Briffa et al., 1996). Once the trend is defined, simply dividing each tree-ring value by the corresponding value of the curve could facilitate its removal from the series (Briffa et al., 1996). Needless to say, an assumption of the approach is that biological age is the only non-climatic factor influencing growth or that non-climatic factors other than tree age remain constant over long periods of time.

Because of these simplifications, the theory of single curve detrending has been suggested to apply with the greatest validity to timberlines, where unusually long distances between the individual trees would exclude much of the ecological disturbances that otherwise influence stem growth, as occurs in more densely forested areas (Fritts, 1976; Briffa et al., 1996; Esper et al., 2002). The image of timberlines as ecologically unchanging open landscapes has, however, proven illusory, with paleobotanical evidence indicating vivid ecotone stand dynamics over the present interglacial (MacDonald et al., 2000; Hiller et al., 2001; Boettger et al., 2003; Kullman, 2005; Mazepa, 2005). A recent lesson has been derived from modern timberlines in which wide-scale advances and concomitant stand densifications are depicted as responses to regional and global warming (Esper and Schweingruber, 2004). If the densifications and thinnings influenced tree-ring growth in ways that significantly altered life-long non-climatic trends (i.e., those trends that paleoclimatologists are obligated to eliminate), then the validity of a simplified theory centered on a single expected ageing curve would diminish over long periods of time, endangering the fidelity of the paleoclimate reconstructions based on such techniques. This outcome was indicated in a previous study combining paleoecological and paleoclimatic interpretations to describe a temporally evolving metamorphosis of tree-ring ageing trends in several hundreds and thousands of tree-ring series over the past millennia (Helama et al., 2005c). Increasing evidence shows spurious changes in tree-ring trend shapes during the late and post-glacial times (Spurk et al., 2002; Naurzbaev et al., 2004; Helama et al., 2005b; Schaub et al., 2008a, b). Moreover, the findings indicated that a slight modification to the previously proposed algorithm to remove the non-climatic growth trends from tree-ring series (Briffa et al., 1996), consisting of a time-dependent adjustment of trend shape due to the changing population density, could actually enhance the paleoclimate signal in the chronology at millennial timescales (Helama et al., 2005c).

These findings guided us to eliminate non-climatic biases from individual tree-ring series in such a way that each tree-ring series was detrended by an ontogenetic model, including two time-independent (juvenile and mature growth level) and one time-dependent (trend concavity) parameters. This approach allowed adjustment for the greatly varying population density that has occurred in that habitat and instantly unearthed climatic signals otherwise overshadowed by timberline population dynamics. Importantly, the exploited temporal variations in past population density and trend shape were in accordance with concomitant variations over spatial scales (Mikola, 1950; Helama et al., 2005a).

**Initial data**

An exhaustive assemblage of dendrochronologically dated Scots pine (*Pinus sylvestris* L.) megafossil stems from subarctic timberline ($N_T$ = 1199) and slightly more southern provenance ($N_S$ = 50) in Lapland (70–68ºN to 30–20ºE) (Eronen et al., 1999, 2002; Helama et al., 2008) was exploited for temporal variations in accumulation rates and tree-ring widths. A set of tree-ring width series from living pines ($N_L$ = 69) from the same region was used to improve the modern part of the tree-ring chronology. Dendrochronological techniques ensured the dating of each ring to the accuracy of the calendar year ($t$). The combined chronology ($N_T$ +$N_S$ +$N_L$) spans over the past 75 centuries and covers the interval -5633 $\leq$ $t \leq$ 2007.

**Temporal instability of sample size**

To portray the chronological variations in sample size ($n$), the tree-ring dataset of timberline megafossils ($N_T$ = 1199) was examined for each calendar year $t$ using a range of –5500 $\leq$ $t \leq$ 1850, which is a time window governed by megafossils (because the assemblage of living pines would not reflect variations in paleoecological conditions). Taphonomic control was previously evaluated secondary to ecological factors in controlling long-term

variations in time-dependent estimates of sample size, $n_t$ (Helama et al., 2005b). We therefore accept $n_t$ directly as a temporally varying measure of past population density (Fig. DR1a). Timescale-dependent behavior in $n_t$ was estimated by applying a set of *s*-year cubic smoothing splines (*s* = 100, 200…1500) (Cook and Peters, 1981) to the data. The time- and timescale-dependent estimate of sample size was denoted as $n_{t,s}$ for each calendar year *t* after smoothing the series by *s*-year spine (Fig. DR1b).

**Quantification of trend**

The tree-ring variability of each stem comprises an ontogenetic trend that is largely controlled by non-climatic factors. This trend is often curvilinear and can be defined as a function of tree age by

$$t_a = je^{-ca} + m, \quad j > 0, c > 0 \qquad \text{(Eq. DR1)}$$

where $t_a$ is the value of the trend in ontogenetic year *a* (in practice, ring number), *j* approximates the level of juvenile growth, *c* controls the trend concavity, and *m* is the mature growth level in an old tree (Fritts et al., 1969). Notably, the trend approaches a straight line and may appear linear with values of *c* approaching zero. Linear trends were modeled by a regression line (because parameterization with $c = 0$ would invalidate Eq. (DR1)), thus accepting zero concavity for these samples. Subsequently, the dataset of timberline megafossil tree rings was examined for ontogenetic trends by (i) determining *c* for each tree and evaluating chronological mean variations of concavity, $c_t$, within the pine population (Fig. DR1c) and (ii) examining timescale-dependent behavior of $c_t$ using a set of *s*-year cubic smoothing splines (*s* = 100, 200…1500; Fig. DR1d). In doing so, we produced time- and timescale-dependent records of $c_{t,s}$ in an identical manner to the quantification of $n_{t,s}$.

**Correlativity of sample size and trend shape**

In principle, $c_{t,s}$ archives tree-ring behavior at timescales exceeding the tree biological age (i.e., segment length, which is on average 167 rings in this study), on multi-centurial to millennial timescales. These variations are by definition extrinsic to tree ageing, and the observed variations in $c_{t,s}$ are thus characteristically environmental or climatic (or noise). Timescale-dependent correlations between $n_{t,s}$ and $c_{t,s}$ are positive and high (Fig. DR2), indicating temporal variations in the concavity of the ontogenetic trend to be related to corresponding variations in timberline population density. They should thus be taken into account when eliminating the non-climatic trends from individual tree-ring series prior to paleoclimatic interpretation. A simulation using the Monte Carlo technique (Efron and Tibshirani, 1986) was applied to test the statistical significance of timescale-dependent correlations between $n_{t,s}$ (shown in Fig. DR1b) and $c_{t,s}$ (shown in Fig. DR1d) by producing a set of 1000 surrogate time-series with an autocorrelation structure similar to that of the spline-smoothed data (the same technique was used in subsequent analyses to estimate the significance for other pairs of series). Correlations appear statistically significant ($P < 0.01$) using $s$ = 800…1100 (Fig. DR2). Thus, the choice of $s = 800$ to de-noise the series by smoothing would be judged by the significant correlation between $n_{t,s}$ and $c_{t,s}$. Moreover, the relatively flexible spline curve allows for more variance than would be provided by the choice of $s$ = 900…1200.

**Detrending the series**

A transient low in $n_t$ is evident during the first millennium BC (especially, $-600 \leq t \leq -100$; Fig. DR1a). To enhance the timberline chronology, tree-ring series from megafossils of slightly more southern provenance ($N_S$ = 50) were included in the chronology of the northern

Finnish Lapland by Eronen et al. (2002). To build the final chronology, these series as well as tree-rings of living pines ($N_L$ = 69) were used ($N_T$ +$N_S$ +$N_L$). Subsequently, we sought for the possibility to enhance the estimation of $c_t$ using the $w$-th Winsorized mean (Fuller, 1991)

$$c_{t,w} = n_t^{-1}\left[\sum_{i=1}^{n_t-w} c_i + c_{n_t-w}w\right] \qquad \text{(Eq. DR2)}$$

which is expected to outweigh the arithmetic mean in skewed data. Correlations between $n_t$ and $c_{t,w}$ were calculated subsequent to smoothing the records by 800-year spline, thus producing timescale-dependent estimates of $n_{t,s}$ and $c_{t,w,s}$ ($s$ = 800). An increase of $w$ improved the temporal correlativity of $n_{t,800}$ and $c_{t,w,800}$ (Table DR1), illustrating that the Winsorized procedure (Eq. DR2) provides a skillful concavity estimate to reveal the relationships between the past population and growth variations, at least on the investigated sample and scales.

Using the previously established regional curve standardization (RCS) (Briffa et al., 1996), all available tree-ring series were averaged and aligned by their ontogenetic years, $a$, subsequently rationalizing the mean curve by an appropriate growth model, such as Eq. DR1. In this study, such time-independent average ageing could be parameterized as

$$t_a = 0.962e^{-0.0178a} + 0.331 \qquad \text{(Eq. DR3)}$$

Crucially, paleontological evidence exemplified that the trend concavity shows considerable environmental variations at multi-centennial to millennial timescales (Fig. DR1c, d). Accordingly, accepting the time-independent $c = 1.78\times10^{-2}$ would introduce non-climatic low-frequency variation into the chronology. Moreover, the Winsorization provided improved

mean estimates for trend concavity, and the use of $c_{t,4,800}$ (i.e., choice of $w$ = 4 and $s$ =800) resulted in time-dependent concavity variations with a long-term level that approximated the time-independent $c = 1.78 \times 10^{-2}$, with $\bar{c}_{t,4,800} = 1.77 \times 10^{-2}$ (Table DR1). Importantly, the temporal variations in $c_{t,4,800}$ correlated with $n_{t,800}$ positively and significantly (Table DR2).

The temporal behavior of $c_{t,4,800}$ was also compared to variations in relative growth rate and juvenile growth. The former was assessed "according to the ratio of the radius of each tree divided by the radius of the single, overall-sample RCS curve at the point corresponding to the final age of that tree" (Briffa and Melvin, 2009). Here, the latter was determined two different ways: as the average ring-width of the first 20 rings in each series $1 < a \leq 20$ (Helama et al., 2005c) and as the maximum ring width value among those 20 rings. The series-specific estimates were computed to mean series and smoothed with 800-year cubic spline (to investigate the scales relevant to exploited scales in the behavior of $c_{t,4,800}$) to portray their temporal population-wise variations (Fig. DR3).

Smoothed records of megafossil sample size and concavity correlated significantly prior and subsequent to simple removal of linear trends from the series (Table DR2). Instead, the relative growth rate and concavity did not correlate with statistical significance either prior or subsequent to removal of linear trends. Moreover, the relative growth rate did not correlate with the sample size variations, implying that the relative growth rate is a measure independent of the concavity and past population density level at relevant scales. The two estimates of juvenile growth correlated strongly with each other, indicating that they are measuring similar phenomena in growth and thus further ensuring the reliability of these estimates. Moreover, the juvenile growth correlated highly with relative growth rate, especially after removal of the trends, evidencing that the juvenile growth is likely the main driver of the variations observed in relative growth rate over the mid and late Holocene.

Concavity did correlate positively but not with statistical significance with juvenile growth level, and only poorly after the removal of the trends (Table DR2). In conclusion, these results implied that the concavity is independent of relative growth rate and juvenile growth (that are actually much more closely related to each other) at relevant timescales (in terms of trend and variations of shorter periods) and that no biasing mechanism (Briffa and Melvin, 2009) can be expected from the use of time-dependent concavity when detrending these data.

The final equation to detrend the tree-ring series can thus be defined as

$$t_a = 0.962e^{-c_{t,4,800}a} + 0.331, \quad 1.10\times10^{-2} \le c_{t,4,800} \le 2.45\times10^{-2} \quad \text{(Eq. DR4)}$$

where $c_{t,4,800}$ is the time- and timescale-dependent concavity estimate during the calendar year ($t$) of the first ring ($a$ = 1) in each series to be detrended. That is, observed (measured) tree-ring values were divided by the value of the curve (Eq. DR4) to derive index series. Subsequently, the indices were averaged into chronology using a bi-weight robust estimation as suggested by Cook (1985).

**Transfer function**

The variance of the tree-ring chronology was stabilized using the method of Osborn et al. (1997), using a time-independent estimate of mean inter-series correlation ($\bar{r} = 0.330$) (Helama et al. 2004c). The chronology was regressed against instrumental climate data from a nearby weather station (Karasjok, northern Norway; 69º28’N; 25º31’E) to depict temperature variations on a Celsius scale. Previous studies have demonstrated site- and time-independent sensitivity of tree-ring growth to mid-summer temperatures (Lindholm et al., 1995; Helama et

al., 2004a; Macias et al., 2004). Mean July temperatures ($1877 \leq t \leq 2004$) were reconstructed using multiple linear regression, where the climate ($C$) in year $t$ was estimated using chronology index ($x$) of previous ($t-2, t-1$), concurrent ($t$), and forthcoming years ($t+1, t+2$). This method was previously evaluated as an appropriate paleoclimatic model for these data (Helama et al., 2009). The transfer function was thus parameterized as

$$C_t = 10.60 - 1.04x_{t-2} - 0.84x_{t-1} + 6.64x_t - 0.64x_{t+1} - 1.50x_{t+2} \quad \text{(Eq. DR5)}$$

Independent verification shows a constant relationship between the records over the separate verification periods (Table DR3). The reduction-of-error statistic (Fritts, 1976) is positive for both sub-periods, indicating skill in the reconstruction (Table DR3). The reconstruction accounts for more than 40% of the total observed variability ($R^2 = 0.43$; $R^2_{ADJ} = 0.41$). The explained variance is even higher, up to 90% at lower frequencies, and the records closely follow each other (Fig. 2 in the main text). Applying Eq. DR5, the tree-ring chronology was metamorphosed into yearly estimates of summer temperatures for $-5500 \leq t \leq 2005$.

**Sunspots and temperatures**

Reconstruction of sunspot numbers ($-9460 \leq t \leq 1900$) was available in decadal resolution (Solanki et al., 2004). The reconstruction was spliced with the decadally averaged group sunspot number record ($1901 \leq t \leq 1990$), based on telescopic observations (Hoyt and Schatten, 1998; Solanki et al., 2004). Prior to comparisons, the temperature reconstruction was sub-sampled to similar (non-overlapping decadal) time-blocks. The series were linearly detrended and transformed into z-scores having a mean of zero and a standard deviation of one prior to analyses. Recent studies have emphasized the importance of two distinct

timescale-dependent modes of variation, those acting on 1000-year and 2500-year scales, in studying the history of the Sun's activity and Holocene climate around the North Atlantic (Nederbragt and Thurow, 2005; Debret et al., 2007). The variations on these scales were separated using *s*-year splines (with a 50% cut-off) with three different frequency responses ($s = 500$, $s = 2000$, $s = 3000$) to the detrended and rescaled reconstructions of temperature and sunspots. Timescale-dependent variations were isolated as the millennial and bi-millennial modes of variability and extracted from the series as residuals (by subtraction) between the 500-year and 2000-year, and 2000-year and 3000-year splines, respectively. Timescale-dependent elements of the reconstructions (temperature and sunspots) were correlated for lags of 0 to 400 years (where sunspots increasingly predate temperatures). Originally, the reconstruction of sunspots (Solanki et al., 2004) was designed to take into account carbon cycle effects (Usoskin and Kromer, 2005); in addition, there was a good correlation with the observed (Hoyt and Schatten, 1998) and reconstructed (Solanki et al., 2004) sunspot numbers without any noticeable temporal shift over the telescopic era. Climatic mechanisms rather than carbon cycle effects could thus be expected to explain potential lagging correlations.

**Spectral estimation**

Multi-taper method (MTM) of Ghil et al. (2002) was applied to the reconstruction. The detection of significant oscillatory modes was carried out using a range of bandwidth parameters ( $p$ ) and number $K$ of tapers (Table DR4). The obtained results were independent of the choice of $p$ and $K$ as the significant oscillatory modes were distinctly similar in length regardless of the choice. This was a clear demonstration of robustness on the spectral estimation and the obtained results of significant climatic periodicities.

**ACKNOWLEDGMENTS**

The sunspot data are available via NOAA Paleoclimatology, downloadable at http://www.ncdc.noaa.gov/paleo/. This study was supported by the Academy of Finland (#122033, 217724).

**REFERENCES CITED**

Boettger, T., Hiller, A., and Kremenetski, K., 2003, Mid-Holocene warming in the northwest Kola Peninsula, Russia: northern pine-limit movement and stable isotope evidence: The Holocene, v. 13, p. 403-410.

Briffa, K.R., and Melvin, T.M., 2009, A closer look at Regional Curve Standardisation of tree-ring records: justification of the need, a warning of some pitfalls, and suggested improvements in its application, in Hughes, M.K., Diaz, H.F., and Swetnam, T.W., Dendroclimatology: Progress and Prospects, Developments in Paleoenvironmental Research 11, Springer Verlag.

Briffa, K.R., Jones, P.D., Schweingruber, F.H., Karlén, W., and Shiyatov, S.G., 1996, Tree-ring variables as proxy-climate indicators: Problems with low-frequency signals, in Jones, P.D., Bradley, R.S., and Jouzel, J., Climatic Variations and Forcing Mechanisms of the Last 2000 Years. NATO ASI Ser., Ser. I, vol. 41, New York, Springer-Verlag, p. 9-41.

Cook, E.R., 1985, A time series analysis approach to tree-ring standardization, [Ph.D. thesis]: Tucson, University of Arizona, 171 p.

Cook, E.R., and Peters, K., 1981, The smoothing spline: a new approach to standardizing forest interior tree-ring width series for dendroclimatic studies: Tree-Ring Bulletin, v. 41, p. 45-53.

Cook, E.R., Briffa, K.R., Meko, D.M., Graybill, D.A., and Funkhouser, G., 1995, The 'segment length curse' in long tree-ring chronology development for palaeoclimatic studies: The Holocene, p. 5, v. 229-237.

Debret, M., Bout-Roumazeilles, V., Grousset, F., Desmet, M., McManus, J.F., Massei, N., Sebag, D., Petit, J.-R., Copard, Y., and Trentesaux, A., 2007, The origin of the 1500-year climate cycles in Holocene North-Atlantic records: Climate of the Past, v. 3, p. 569-575.

Efron, B., and Tibshirani, R., 1986, Bootstrap Methods for Standard Errors, Confidence Intervals, and Other Measures of Statistical Accuracy: Statistical Science, v. 1, p. 54-75.

Eronen, M., Hyvärinen, H., and Zetterberg, P., 1999, Holocene humidity changes in northern Finnish Lapland inferred from lake sediments and submerged Scots pines dated by tree rings: The Holocene, v. 9, p. 569-580.

Eronen, M., Zetterberg, P., Briffa, K.R., Lindholm, M., Meriläinen, J., and Timonen, M., 2002, The supra-long Scots pine tree-ring record for Finnish Lapland: part 1, chronology construction and initial references: The Holocene, v. 12, p. 673-680.

Esper, J., and Schweingruber, F.H., 2004, Large-scale treeline changes recorded in Siberia. Geophysical Research Letters, v. 31, doi: 10.1029/2003GL019178.

Esper, J., Cook, E.R., and Schweingruber, F.H., 2002, Low-frequency signals in long tree-line chronologies for reconstructing past temperature variability: Science, v. 295, p. 2250-2253.

Fritts, H.C., 1976, Tree Rings and Climate: London, Academic Press, 567 p.

Fritts, H.C., Mosimann, J.E., and Bottorff, C.P., 1969, A revised computer program for standardizing tree-ring series: Tree-Ring Bulletin, v. 29, p. 15-20.

Fuller, W.A., 1991, Simple estimators for the mean of skewed populations: Statistica Sinica, v. 1, p. 137-158.

Ghil, M., Allen, M.R., Dettinger, M.D., Ide, K., Kondrashov, D., Mann, M.E., Robertson, A.W., Saunders, A., Tian, Y., Varadi, F., and Yiou, P., 2002, Advanced spectral methods for climatic time series: Reviews of Geophysics, v. 40, doi:10.1029/2000RG000092.

Helama, S., Lindholm, M., Meriläinen, J., Timonen, M., and Eronen, M., 2005a, Multicentennial ring-width chronologies of Scots pine along north-south gradient across Finland: Tree-Ring Research, v. 61, p. 21-32.

Helama, S., Lindholm, M., Timonen, M., and Eronen M., 2004b, Dendrochronologically dated changes in the limit of pine in northernmost Finland during the past 7.5 millennia: Boreas, v. 33, p. 250-259.

Helama, S., Lindholm, M., Timonen, M., and Eronen, M., 2004c, Detection of climate signal in dendrochronological data analysis: a comparison of tree-ring standardization methods: Theoretical and Applied Climatology, v. 79, p. 239-254.

Helama, S., Lindholm, M., Timonen, M., and Eronen, M., 2005b, Mid- and late Holocene tree population density changes in northern Fennoscandia derived by a new method using megafossil pines and their tree-ring series: Journal of Quaternary Science, v. 20, p. 567-575.

Helama, S., Makarenko, N.G., Karimova, L.M., Kruglun, O.A., Timonen, M., Holopainen, J., Meriläinen, J., and Eronen, M., 2009, Dendroclimatic transfer functions revisited: Little Ice Age and Medieval Warm Period summer temperatures reconstructed using artificial neural networks and linear algorithms: Annales Geophysicae, v. 27, p. 1097-1111.

Helama, S., Mielikäinen, K., Timonen, M., and Eronen M., 2008, Finnish supra-long tree-ring chronology extended to 5634 BC: Norwegian Journal of Geography, v. 62, p. 271-277.

Helama, S., Timonen, M., Lindholm, M. Meriläinen, J., and Eronen, M., 2005c, Extracting long-period climate fluctuations from tree-ring chronologies over timescales of centuries to millennia: International Journal of Climatology, v. 25, p. 1767-1779.

Helama, S., Holopainen, J., Timonen, M., Ogurtsov, M. G., Lindholm, M., Meriläinen, J., and Eronen, M., 2004a, Comparison of living-tree and subfossil ring-widths with summer temperatures from 18th, 19th and 20th centuries in northern Finland: Dendrochronologia, v. 21, p. 147-154.

Hiller, A., Boettger, T., and Kremenetski, C., 2001, Medieval climate warming recorded by radiocarbon dated alpine tree-line shift on the Kola Peninsula, Russia: The Holocene, v. 11, p. 491-497.

Hoyt, D.V., and Schatten, K.H., 1998, Group sunspot numbers: A new solar activity reconstruction. Solar Physics, v. 179, p. 189-219.

Kullman, L., 2005, Pine (*Pinus sylvestris*) treeline dynamics during the past millennium - a population study in west central Sweden: Annales Botanici Fennici, v. 42, p. 95-106.

Lindholm, M., Eronen, M., Meriläinen, J., and Zetterberg, P., 1995, A tree-ring record of past summer temperatures in northern Finnish Lapland: Fennoscandia archaeologica, v. 12, p. 95-101.

MacDonald, G.M., Gervais, B.R., Snyder, J.A., Tarasov, G.A., and Borisova, O.K., 2000, Radiocarbon dated *Pinus sylvestris* L. wood from beyond tree line on the Kola Peninsula, Russia: The Holocene, v. 10, p. 143-147.

Macias, M., Timonen, M., Kirchhefer, A., Lindholm, M., Eronen, M. and Gutiérrez, E., 2004, Growth variability of Scots pine (*Pinus sylvestris*) along a west-east gradient across northern Fennoscandia: A dendroclimatic approach: Arctic, Antarctic and Alpine Research, v. 36, p. 565-574.

Mazepa, V.S., 2005, Stand density in the last millennium at the upper tree-line ecotone in the Polar Ural Mountains: Canadian Journal of Forest Research, v. 35, p. 2082-2091.

Mikola, P., 1950, On variations in tree growth and their significance to growth studies: Communicationes Instituti Forestalis Fenniae, v. 38, p. 1-131.

Naurzbaev, M.M., Hughes, M.K. and Vaganov, E.A., 2004, Tree-ring growth curves as sources of climatic information: Quaternary Research, v. 62, p. 126-133.

Nederbragt, A.J., and Thurow, J., 2005, Geographic coherence of millennial-scale climate cycles during the Holocene: Palaeogeography, palaeoclimatology, palaeoecology, v. 221, p. 313-324.

Osborn, T.J., Briffa, K.R., and Jones, P.D., 1997, Adjusting variance for sample size in tree-ring chronologies and other regional mean timeseries: Dendrochronologia, v. 15, p. 89-99.

Schaub, M., Büntgen, U., Kaiser, K.F., Kromer, B., Talamo, S., Andersen, K.K., and Rasmussen, S.O., 2008a, Lateglacial environmental variability from Swiss tree rings: Quaternary Science Reviews, v. 27, p. 29-41.

Schaub, M., Kaiser, K.F., Frank, D.C., Büntgen, U., Kromer, B., and Talamo, S., 2008b, Environmental change during the Allerød and Younger Dryas reconstructed from Swiss tree-ring data. Boreas, v. 37, p. 74-86.

Solanki, S.K., Usoskin, I.G., Kromer, B., Schüssler, M., and Beer, J., 2004, Unusual activity of the Sun during recent decades compared to the previous 11,000 years: Nature, v. 431, p. 1084-1087.

Spurk, M., Leuschner, H.H., Baillie, M.G.L., Briffa, K.R., and Friedrich, M., 2002, Depositional frequency of German subfossil oaks: climatically and non-climatically induced fluctuations in the Holocene: The Holocene, v. 12, p. 707-715.

Stuiver, M., Reimer, P.J., Bard, E., Beck, J.W., Burr, G.S., Hughen, K.A., Kromer, B., McCormac, G., van der Plicht, J., and Spurk, M., 1998, NTCAL98 radiocarbon age calibration, 24,000-0 cal BP: Radiocarbon, v. 40, p. 1041-1083.

Usoskin, I.G., and Kromer, B., 2005, Reconstruction of the 14C production rate from measured relative abundance: Radiocarbon, v. 47, p. 31-37.

Vaganov, E.A., Hugher, M.K., and Shashkin, A.V., 2006, Growth Dynamics of Conifer Tree Rings - Images of Past and Future Environments: Ecological Studies, v. 183, p. 1-354.

**TABLE DR1.** Temporal estimation of concavity variations with correlations to sample size.

| *Winsorization*[1] | 1 | 2 | 3 | 4 | 5 |
|---|---|---|---|---|---|
| Correlation[2] | 0.193 | 0.398 | 0.489 | 0.566 | 0.642 |
| Mean concavity[3] | 2.126 | 1.979 | 1.861 | 1.770 | 1.678 |

[1]The relationships between *w*-th Winsorized $c_{t,w,800}$ (Eq. DR2) and $n_{t,800}$ of megafossils were compared.

[2]Pearson correlation between $c_{t,w,800}$ and $n_{t,800}$ were calculated over the period of megafossil governance ($-5500 \le t \le 1850$).

[3]The grand mean time-dependent concavity ($\bar{c}_{t,w} \times 10^{-2}$) over the study period ($-5500 \le t \le 2007$) approximates the time-independent estimate of $c = 1.78 \times 10^{-2}$ (Eq. DR3) over the same period, when $w = 4$.

**TABLE DR2.** Pearson correlations between the temporal variations in the sample size of megafossils, their growth trend concavities, relative growth rate, and juvenile growth.

**(A)**

| *Before detrending*[1] | Sample size | Concavity | Relative growth rate | Juvenile growth (average) | Juvenile growth (maximum) |
|---|---|---|---|---|---|
| Sample size[2] | 1 | | | | |
| Concavity[3] | 0.556** | 1 | | | |
| Relative growth rate[4] | -0.265 | -0.292 | 1 | | |
| Juvenile growth (average)[5] | -0.010 | 0.408 | 0.360 | 1 | |
| Juvenile growth (maximum)[6] | 0.075 | 0.451 | 0.288 | 0.972** | 1 |

**(B)**

| *After detrending*[7] | Sample size | Concavity | Relative growth rate | Juvenile growth (average) | Juvenile growth (maximum) |
|---|---|---|---|---|---|
| Sample size | 1 | | | | |
| Concavity | 0.573** | 1 | | | |
| Relative growth rate | -0.260 | -0.076 | 1 | | |
| Juvenile growth (average) | -0.058 | 0.259 | 0.821** | 1 | |
| Juvenile growth (maximum) | 0.034 | 0.287 | 0.814** | 0.967** | 1 |

[1]Similarly smoothed records were compared (see Fig. DR2a–e) and statistically significant correlations are denoted as asterisks (** $P < 0.01$; * $P < 0.05$).

[2]Determined as $n_{t,800}$, $-5500 \le t \le 1850$.

[3]Determined as $c_{t,4,800}$, $-5500 \le t \le 2007$.

[4]Determined as a ratio of the radius of each tree divided by the radius of the single, overall-sample RCS curve.

[5]Determined as an arithmetic mean of the first 20 ring widths of each tree ($1 < a \le 20$).

[6]Determined as the maximum ring width value among the first 20 rings of each tree ($1 < a \le 20$).

[7]The smoothed records were linearly detrended and compared (see Fig. DR2f–j).

**TABLE DR3.** Calibration and verification statistics for the temperature reconstruction.

| *Calibration period*[1] | 1877–1940 | 1941–2004 | 1877–2004 |
|---|---|---|---|
| *Verification period* | 1941–2004 | 1877–1940 | |
| Calibration | | | |
| Pearson correlation | 0.712 | 0.626 | 0.657 |
| Verification | | | |
| Pearson correlation | 0.559 | 0.632 | |
| Reduction of error | 0.323 | 0.184 | |

[1]The calibration period was divided into two sub-periods for cross-validation to ensure the reliability of the transfer function (Eq. DR5).

**TABLE DR4.** Robustness of significant oscillatory modes in the temperature reconstruction. The analysis was carried out using the multi-taper method.

| $p$[1] | $K$[2] | Period[3] | Significance[4] |
|---|---|---|---|
| 3 | 5 | 234 | 90 |
| 3 | 5 | 134 | 99 |
| 3 | 5 | 109 | 95 |
| 4 | 7 | 228 | 95 |
| 4 | 7 | 132 | 99 |
| 4 | 7 | 108 | 95 |
| 5 | 9 | 221 | 95 |
| 5 | 9 | 139 | 99 |
| 5 | 9 | 106 | 95 |
| 6 | 11 | 216 | 95 |
| 6 | 11 | 137 | 95 |
| 6 | 11 | 102 | 95 |

[1]The bandwidth parameter.

[2]The number of tapers.

[3]Lenght of the periodic oscillation in years.

[4]Indicates that the mode is significant at the 90, 95 or 99 % level against a null hypothesis of red noise.

**FIGURE CAPTIONS**

**Figure DR1.** Temporal behavior in sample size and concavity of trends. Sample size of timberline megafossils, $n_t$ (a) and $n_{t,s}$ (b), and the tree-ring based growth trend concavities, $c_t$ (c) and $c_{t,s}$ (d), are compared over the period of megafossils governance (here, $-5500 \le t \le 1850$). Original series (a, c) were smoothed by *s*-year cubic splines (*s* = 100, 200…1500). Statistical relationships between the series are quantified in Fig. DR2.

**Figure DR2.** Statistical relationships between sample size and concavity of trends. Timescale-dependent sample size of timberline megafossils, $n_{t,s}$ and their tree-ring–based growth trend concavities, $c_{t,s}$, were evaluated statistically using Pearson correlations after applying *s*-year spline to original data. Significant ($P < 0.01$) correlations are indicated as gray histograms.

**Figure DR3.** Visual comparison of chronology characteristics. The variations in the sample size of megafossils (a), growth trend concavity (b), relative growth rate (c), and juvenile growth level determined as average (d) and maximum values (e) of the first 20 ring widths, depicted as thick lines. Series were smoothed by 800-year spline. Their linear trends (regression line; thin line) were further removed to detrend the series (f–j).

# Figure DR1

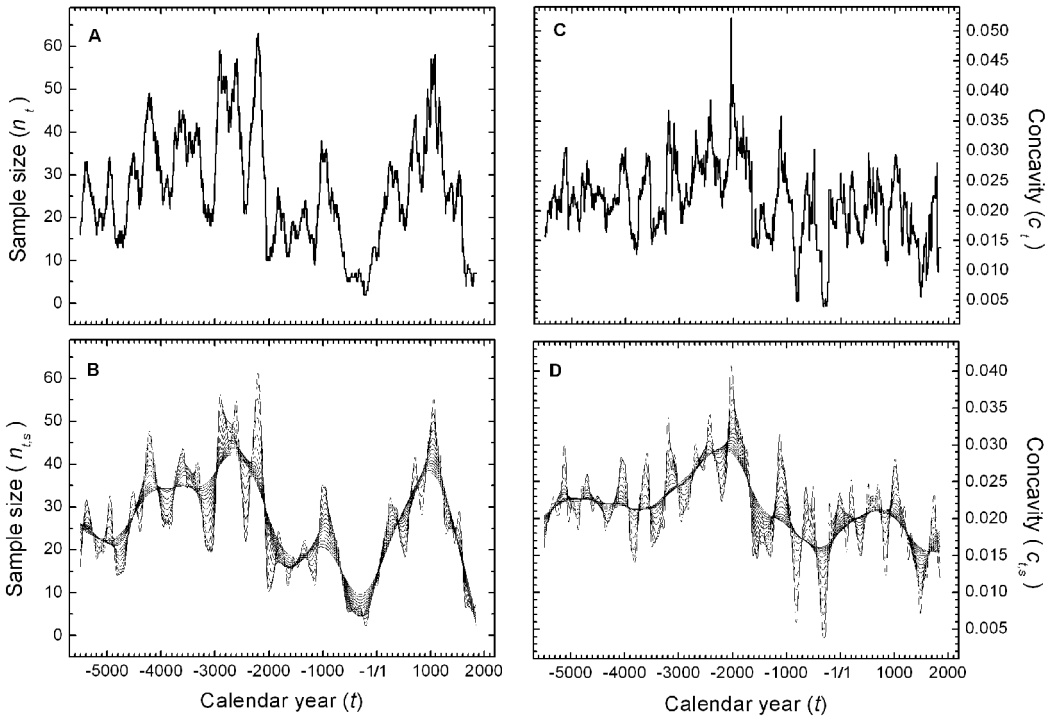
A
B
C
D
Sample size ($n_t$)
Sample size ($n_{t,s}$)
Concavity ($c_t$)
Concavity ($c_{t,s}$)
Calendar year ($t$)
Calendar year ($t$)
-5000 -4000 -3000 -2000 -1000 -1/1 1000 2000

**FIGURE DR2**

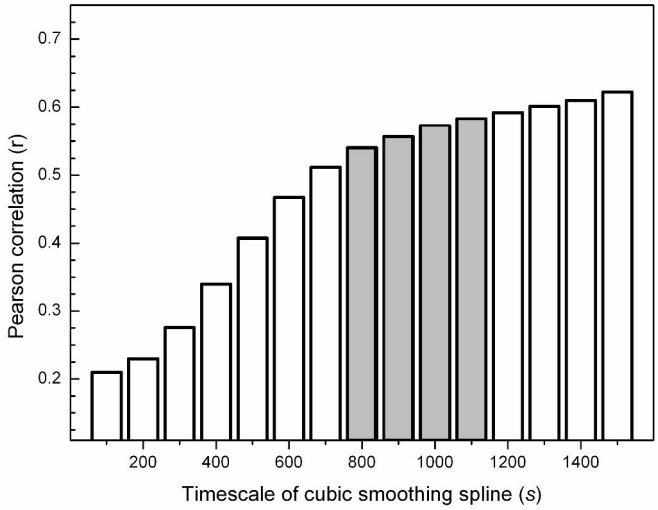
Pearson correlation (r)
0.7
0.6
0.5
0.4
0.3
0.2
200
400
600
800
1000
1200
1400
Timescale of cubic smoothing spline (s)

# FIGURE DR3

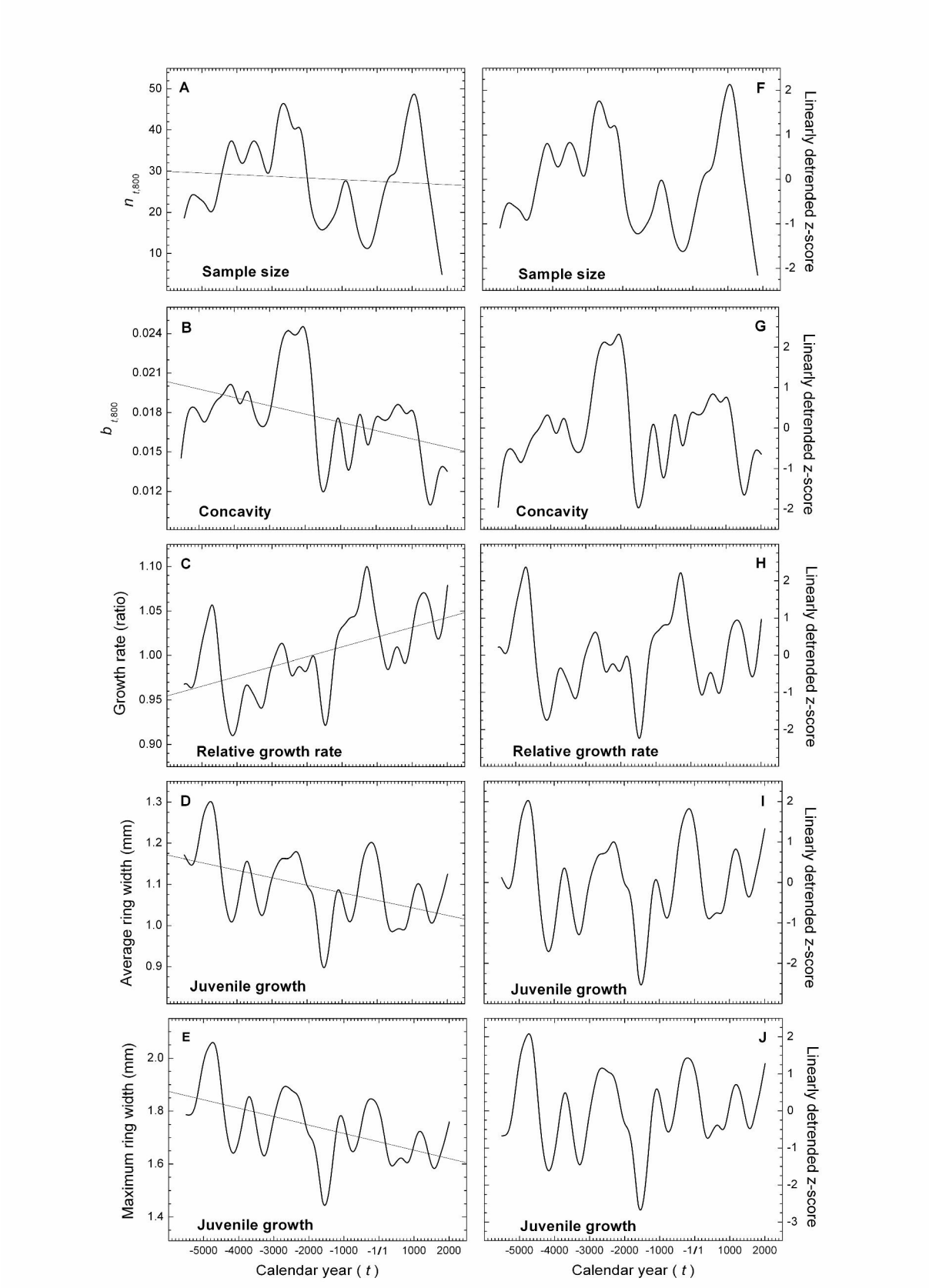
A
B
C
D
E
F
G
H
I
J
Sample size
Concavity
Relative growth rate
Juvenile growth
Juvenile growth
Sample size
Concavity
Relative growth rate
Juvenile growth
Juvenile growth
n 1,800
b 1,800
Growth rate (ratio)
Average ring width (mm)
Maximum ring width (mm)
Linearly detrended z-score
Calendar year ( t )
Calendar year ( t )
-5000 -4000 -3000 -2000 -1000 -1/1 1000 2000